Full Dissolution of the Whole Lithium Sulfide Family (Li$_2$S$_8$ to Li$_2$S) in a Safe Eutectic Solvent for Rechargeable Lithium–Sulfur Batteries

Qian Cheng[+], Weiheng Xu[+], Shiyi Qin, Subhabrata Das, Tianwei Jin, Aijun Li, Alex Ceng Li, Boyu Qie, Pengcheng Yao, Haowei Zhai, Changmin Shi, Xin Yong, and Yuan Yang*

Abstract: *The lithium–sulfur battery is an attractive option for next-generation energy storage owing to its much higher theoretical energy density than state-of-the-art lithium-ion batteries. However, the massive volume changes of the sulfur cathode and the uncontrollable deposition of Li$_2$S$_2$/Li$_2$S significantly deteriorate cycling life and increase voltage polarization. To address these challenges, we develop an ε-caprolactam/acetamide based eutectic-solvent electrolyte, which can dissolve all lithium polysulfides and lithium sulfide (Li$_2$S$_8$–Li$_2$S). With this new electrolyte, high specific capacity (1360 mAh g^{-1}) and reasonable cycling stability are achieved. Moreover, in contrast to conventional ether electrolyte with a low flash point (ca. 2°C), such low-cost eutectic-solvent-based electrolyte is difficult to ignite, and thus can dramatically enhance battery safety. This research provides a new approach to improving lithium–sulfur batteries in aspects of both safety and performance.*

Lithium–sulfur batteries are promising candidates for next-generation energy-storage systems,[1] as they have a high theoretical specific energy density of 2500 Wh kg^{-1}. In Li–S batteries, sulfur undergoes a two-electron process, which results in a high specific capacity of 1675 mAh g^{-1}. However, this two-electron process includes multiple steps, ranging from solid sulfur to soluble long-chain polysulfides (Li$_2$S$_8$, Li$_2$S$_6$, and Li$_2$S$_4$), and precipitation of solid Li$_2$S/Li$_2$S$_2$.[2] Such a complicated process results in multiple mechanisms that deteriorate cycling performance, such as the shuttle effect, random deposition of insulating Li$_2$S, and large volume change.[3] Significant efforts have been devoted to trapping

soluble polysulfides to mitigate their diffusion and the shuttle effect, including confined carbon frameworks,[4] electrode additives,[5] and physical/chemical adsorptions.[6] On the other hand, much less attention has been paid to Li$_2$S$_2$ and Li$_2$S, which count for three-quarters of the total theoretical capacity. The random deposition of insulating Li$_2$S$_2$/Li$_2$S causes large voltage polarization and suppresses continuous reduction of polysulfides, which drastically reduces charge capacity (Figure 1a). The massive volume change (infinite
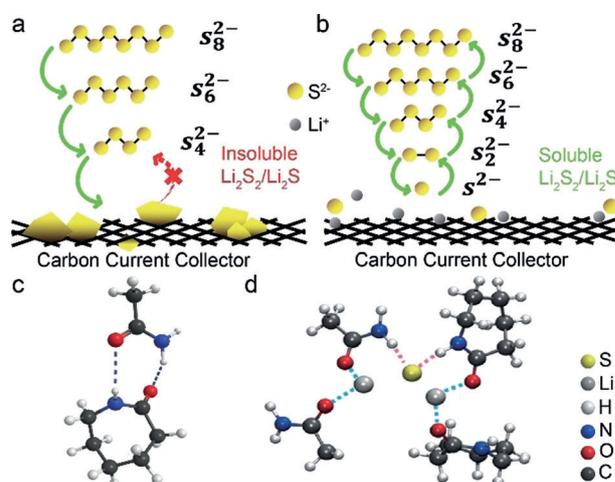
Figure 1. a) Conventional lithium–sulfur batteries with "dead" Li$_2$S/Li$_2$S$_2$ precipitated none-uniformly. b) The proposed structure with all the lithium polysulfides/sulfide soluble. c) The CPL/acetamide mixture bounded by intermolecular hydrogen bond. d) A hypothetical dynamic solvation structure which involves multiple solvent molecules to dissolve Li$_2$S. Dashed lines mark the intermolecular interactions.

from polysulfides to sulfide) also causes pulverization and mechanical failure of electrode materials.[7] This problem is more severe in cells with lean electrolyte, which is necessary for the practical application of Li–S batteries. Recently, it has been shown that modification of carbon electrodes to form uniform Li$_2$S$_2$/Li$_2$S deposition is a practical approach to mitigating these issues.[8]

A feasible alternative approach to solving these issues is to render Li$_2$S$_2$/Li$_2$S soluble, so that neither solid deposition nor mechanical stress will occur during battery cycling and thus stable cycling can be expected. The solubility may also help reduce the non-uniform deposition of Li$_2$S/Li$_2$S$_2$ in conventional Li–S batteries. Recently, NH$_4$-based additive was reported to enhance the dissolution of Li$_2$S in the electrolyte, improving the cycling performance of Li–S batteries with lean electrolyte.[9]

[*] Dr. Q. Cheng,[+] W. Xu,[+] T. Jin, A. J. Li, A. C. Li, B. Qie, P. Yao, H. Zhai,
C. Shi, Prof. Y. Yang
Program of Materials Science and Engineering
Department of Applied Physics and Applied Mathematics
Columbia University
500 W 120th St, New York, NY 10027 (USA)
E-mail: yy2664@columbia.edu

S. Qin, Prof. X. Yong
Department of Mechanical Engineering
The State University of New York, Binghamton
85 Murray Hill Rd. Suite 1300, Rm#1320, Binghamton, NY 13902
(USA)

S. Das
Langmuir Center of Colloids and Interfaces, Columbia University
500 W 120th St, New York, NY 10027 (USA)

[+] These authors contributed equally to this work.

Supporting information and the ORCID identification number(s) for the author(s) of this article can be found under:
https://doi.org/10.1002/anie.201812611.

Herein we present a new eutectic solvent consisting of ε-caprolactam (CPL) and acetamide, which can dissolve all polysulfides and sulfide (Li_2S_8 to Li_2S) to address the above issues (Figure 1b). A high specific capacity of 1360 mAh g^{-1} is achieved at 0.1 C (165 mA g^{-1}), and the capacity remains at 1193 mAh g^{-1} over 40 cycles. With further addition of TiO_2, capacity decay of only 0.15%/cycle over 200 cycles is achieved. Moreover, this eutectic electrolyte does not ignite in contact with fire, in contrast to immediate ignition of the conventional 1,3-dioxolane/1,2-dimethoxyethane (DOL/DME) electrolyte (flash point of 2°C[10]). In addition, its cost (ca. $2–3 kg^{-1}) is significantly less than nonflammable ionic liquids and solid electrolytes.[11]

CPL and acetamide have melting points of 68°C and 80°C, respectively. However, due to the breaking of intra-molecular hydrogen bonds and subsequent reforming of intermolecular hydrogen bonds,[12] their mixture at a 1:1 molar ratio form a clear liquid with a low melting point of −8°C (Figure 1c). These two solvents also have high dielectric constants of 59 and 14 in the liquid state,[13] respectively; thus they have been used to dissolve various polar gas molecules, such as H_2S and SO_2.[12a] Solubility tests show that up to 0.7 M Li_2S can be dissolved in this solvent at room temperature, and the solution is stable even after two months (Figure S1 in the Supporting Information). In contrast, the solubility of Li_2S in the DOL/DME electrolyte is negligible (Figure S2). To exclude the possibility of forming Li_2S colloidal suspension, a Tyndall effect test was conducted on both the pure and 0.4 M Li_2S dissolved eutectic solvent, with 0.2 mg mL^{-1} graphene oxide dispersion as a control sample (Figure 2a). Negligible scattering was observed in both solutions (Figure S3). Besides Li_2S, such solvent also shows good solubility for Li_2S_2 to Li_2S_8 with no precipitation over 400 hours (Figure 2b). The solubility of Li_2S_x is roughly a constant (0.7 M) based on the molarity of the anion (Figure S4). This means that more sulfur can be dissolved for polysulfides (up to 5.6 M for Li_2S_8). The full dissociation of Li-S is also supported by Raman spectra, where the signature peak of Li_2S at 375 cm^{-1} vanishes in 0.4 M Li_2S in the eutectic solvent (Figure 2c and Figure S5).

To understand the dissolution of Li_2S in the eutectic solvent, we performed ab initio molecular dynamics (AIMD) simulations for 0.4 M Li_2S in CPL/acetamide and in DOL/DME (Supporting Information, Note 1). The results show that the dissociation of Li_2S can be attributed to both strong interactions between S^{2-} and the amide hydrogen (N−H), and between Li^+ and carbonyl oxygen atom in the eutectic solvent (C=O; Figure 2d,e). Firstly, the intimate interaction between sulfur and the amide hydrogen is reflected by a sharp peak at 2 Å in the radial distribution function (RDF), which is absent in DOL/DME (Figure 2d). The amide hydrogen is highly electropositive, which can serve as a hydrogen bond donor (Figure S6). These simulation results are consolidated by Raman spectra, showing a new peak at 2572 cm^{-1} corresponding to the H−S stretching mode (Figure 2c).[14] The formation of H−S bond as indicated by an NMR resonance signal at 2.0 ppm[15] is also observed (Figure 2e and Figure S7).
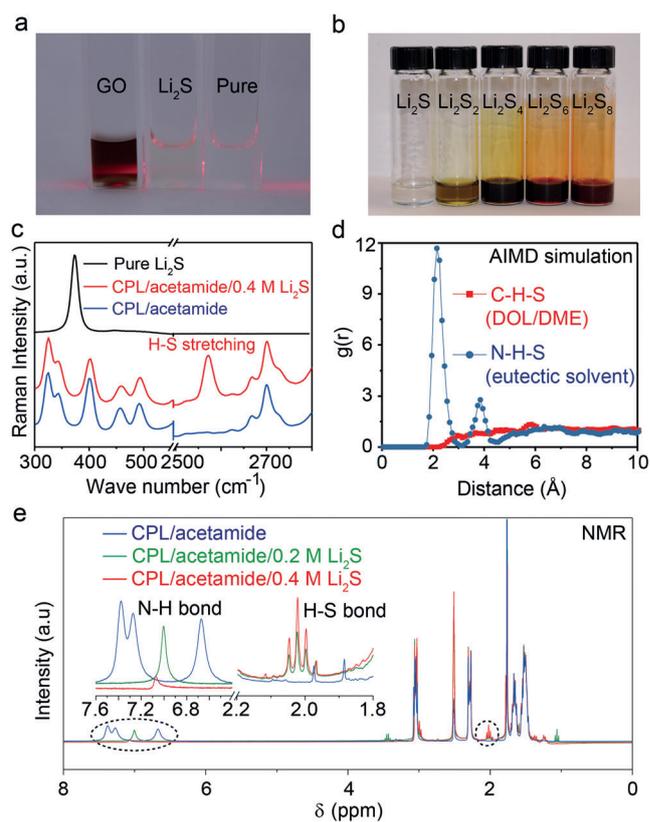
Figure 2. a) Tyndall effect test shows no precipitation or colloids in 0.4 M Li_2S/CPL/acetamide solution. Pure CPL/acetamide and GO dispersion are used as control samples. b) The dissolution of all polysulfides and sulfide in CPL/acetamide. The concentration of S is 0.4 M in all samples. c) Raman spectra of pure Li_2S, CPL/acetamide, 0.4 M Li_2S/CPL/acetamide. d) AIMD simulations show the radial distribution functions between sulfur and the hydrogen in N−H for 0.4 M Li_2S in CPL/acetamide and C−H for DOL/DME. e) NMR spectra of pure eutectic solvent, 0.2 M/0.4 M Li_2S in eutectic solvent. The inset shows spectral features indicating that the S−H bond forms and N−H bond weakens.

The strong interaction between Li^+ and carbonyl oxygen atom is reflected by the strong Li−O peak at 2 Å in RDF, much weaker in the Li_2S/DOL/DME system (Figure S8). This is likely a result of the carbonyl oxygen atom being more electronegative than the oxygen atom in ethers (Figure S6). The stronger interactions between S^{2-} and N−H, and Li^+ and carbonyl oxygen also lead to longer Li−S distance (Figure S9). Due to limited computational power, Li−S does not dissociate during the simulation period of 15 ps, but the Li−S distance in eutectic solvent is indeed longer than that in DOL/DME, and keeps increasing in the simulation (0.01 Å ps^{-1}), which proves that the eutectic solvent can better dissolve Li_2S.

Li_2S dissolved in CPL/acetamide catholyte can be combined with lithium metal, but its viscosity (12 Pa s) is too high to demonstrate high electrochemical performance (Supporting Information, Note 2). Therefore, this eutectic solvent is mixed with DOL/DME at a weight ratio of 1.55:1 to obtain a balance between Li_2S solubility, viscosity, and non-flammability, and Li_2S is 0.2 M in the final catholyte. The addition of DOL/DME into the eutectic solvent does not affect the

2 **www.angewandte.org**

© 2019 Wiley-VCH Verlag GmbH & Co. KGaA, Weinheim

Angew. Chem. Int. Ed. **2019**, *58*, 1–6

◄◄ These are not the final page numbers!

solubility of Li_2S_x inside the eutectic solvent (Figure S10). 1.2 M lithium bis(trifluoromethanesulfonyl) imide (LiTFSI) and 0.1 M $LiNO_3$ are also added to enhance ionic conductivity and passivate lithium surface, respectively. The acquired catholyte (Catholyte$_{eut}$) has a viscosity of 1.4×10^{-2} Pa s and a conductivity of 2.5×10^{-3} S cm^{-1}, together with high stability (Figure S11).

The Catholyte$_{eut}$ is difficult to ignite even with separator presented, demonstrating its low flammability (Figure 3 and Supporting Video). Thermogravimetric analysis shows that
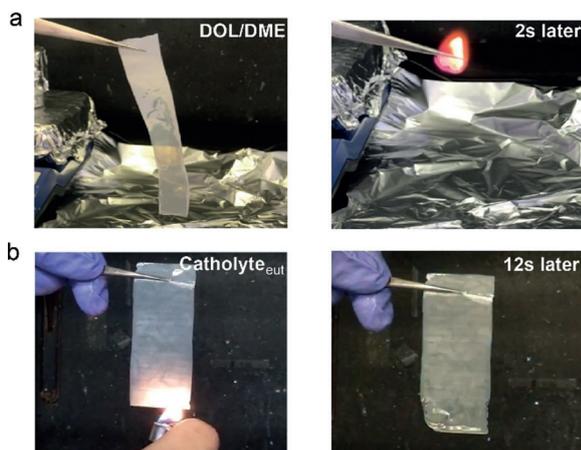
Figure 3. Flammability tests of polypropylene/polyethylene separators soaked with different electrolytes. a) A separator soaked with pure DOL/DME can be readily ignited. b) A separator soaked with the Catholyte$_{eut}$ shows low flammability. See Supporting Video for more details.

Figure 4. Electrochemical performance of 0.2 M Li_2S in the Catholyte$_{eut}$ for Li–S batteries. a) Charge/discharge voltage profiles and b) Cycling performance at 0.1, 0.3 and 0.5 C. c) Electrochemical impedance spectroscopy of the cell charged to 2.3 V at 1st, 5th, 20th, and 40th cycles, corresponding to Li_2S_2 phase. 1 C = 1650 mA g^{-1} sulfur for all data. d) Rate performance test. e) Cycling performance of the TiO_2 coated carbon current collector at 0.3 C.

the Catholyte$_{eut}$ evaporates slowly upon heating, which is the key to their high resistance to ignition (Figure S12 and Supporting Information, Note 3). The Catholyte$_{eut}$ also shows reasonable stability against lithium metal. A Li/Li cell with Catholyte$_{eut}$ shows steady cycling for over 500 hours at 0.3 mA cm^{-2} without increased overpotential (Figure S13), and no dendrites were observed after cycling (Figure S14). X-ray photoelectron spectroscopy proves the existence of a double-layer solid electrolyte interphase (SEI) structure which can protect the lithium metal and minimize the shuttle effect (Supporting Information, Note 4 and Figure S15). In addition, the catholyte without Li_2S shows no redox activity between 1.8 and 2.8 V versus Li/Li$^+$, indicating electrochemical stability in this voltage window (Figure S16).

Next, the Catholyte$_{eut}$ was tested with lithium metal to evaluate battery performance. Since the solubility of S_8 in eutectic solvent is only 0.12 M, the charging cut-off voltage is 2.7 V to keep the amount of generated sulfur below this solubility and avoid the precipitation of solid sulfur, which has adverse effects on cycling performance. The voltage profile shows two plateaus corresponding to high-order polysulfides and Li_2S_2/Li_2S (Figure 4a). At 0.1 C (165 mAh g^{-1}), the specific capacity based on sulfur mass reaches 1258 mAh g^{-1} in the first cycle, then slowly increases to 1360 mAh g^{-1} (Figure 4b). The average discharge potential is 2.21 V, 90 mV higher than that of Li_2S_6 in conventional catholyte

(Catholyte$_{conv}$, Supporting Information, Note 5). The open-circuited voltages of Li_2S_x ($x = 1,2,3,4,6$) in Catholyte$_{eut}$ are also plotted in Figure S17, which are higher than those in DOL/DME. Moreover, the voltage plateau transition happens around Li_2S_3, different from DOL/DME. This is probably caused by the full dissolution from Li_2S_8 to Li_2S, while in DOL/DME the solid–liquid transition may change the redox potential. After 40 cycles, the capacity remains at 1193 mAh g^{-1}, 94.8 % compared to the first cycle. Such retention is higher than 78.8 % of Li_2S_6 in conventional DOL/DME catholyte as our strategy alleviates the random deposition of dead Li_2S/Li_2S_2 and voltage polarization (Figure S18). Electrochemical impedance spectroscopy shows that the charge transfer resistance slightly decreases over cycles (Figure 4c), which could arise from better wetting between Catholyte$_{eut}$ and carbon electrode. The dissolution of Li_2S and Li_2S_2 in cycling is further confirmed by energy dispersive X-ray spectroscopy and SEM. No precipitation of Li_2S was observed on the carbon substrate after cycling (Figure S19), compared to the random Li_2S deposition in the conventional DOL/DME catholyte (Figure S20). Such performance is better than the previous study using ammonium salt to dissolve Li_2S,[9a] and other studies without nanoscale electrode modifications.[2a, 4a, 7a, 9a, 16]

At higher rates of 0.3 and 0.5 C, the initial capacities are 953 and 531 mAh g^{-1}, with capacity retentions of 90.3% and 94.8% after 40 cycles, respectively (Figure 4b). Longer cycling data is presented in Figure S21. The average coulombic efficiencies of all three rates are above 99% (Figure S22), which proves that shuttle effect barely takes place. The shuttling effect is not worse compared to the DOL/DME electrolyte since Li$_2$S is already the most reduced states and the SEI on lithium surface is stable in eutectic solvent (Supporting Information, Note 4). Figure 4d shows that the capacity gradually steps down with increasing current density. At 1 C, the capacity is only around 215 mAh g^{-1}, which is inferior to conventional lithium–sulfur batteries.[8a,16,17] This may originate from the catholyte's high viscosity and low conductivity (Table S1). Such issues can be addressed by further optimizing the electrolyte, or electrode designs to reduce its tortuosity.[18]

The electrochemical performance can be further enhanced by adding electrode additives to confine the dissolved species, which could minimize side reactions with the lithium anode.[5,19] As a demonstration, TiO$_2$ nanoparticles are coated onto the carbon current collector through a previously reported dip-dry method.[5c] The initial capacity is 710 mAh g^{-1} at 0.3 C (495 mA g^{-1}). After a stabilization period of 20 cycles, the capacity drops slowly from 636 to 482 mAh g^{-1} from cycle 20 to 200, representing a decay of only 0.15%/cycle (Figure 4e). The corresponding average CE is 99.5% without shuttle effect. Such results indicate that the system can be further optimized to enhance cycling performance.

In conclusion, we have developed a new safe electrolyte based on ε-caprolactam/acetamide for rechargeable Li–S batteries. Such an electrolyte can dissolve all sulfide and polysulfide species. Therefore, major issues associated with Li$_2$S/Li$_2$S$_2$, such as volume expansion, uncontrollable deposition, and voltage polarization, can be mitigated. Li–S batteries with this new electrolyte reach a capacity of 1360 mAh g^{-1} at 0.1 C with 94.8% capacity retention after 40 cycles. Moreover, this new electrolyte shows high stability against fire to improve the safety of Li–S batteries, which is important but rarely discussed in the Li–S system. Furthermore, CPL/acetamide is only one example of a eutectic solvent.[12a,20] Other combinations (e.g. CPL/imidazole and acetamide/tetrabutylammonium bromide) are all capable of dissolving Li$_2$S (Figure S23). It should be noticed that our studies are based on polysulfide/sulfide electrolyte, which is suitable for semi-flow Li-polysulfide batteries as grid-level energy storage, but further studies with high-mass-loading solid sulfur electrode and lean electrolyte are needed to evaluate the performance for Li–S batteries with high energy density. This provides a large space for developing new electrolytes to increase the solubility of all sulfur species, and to improve safety, energy density, and cycling performance of Li–S batteries.

[1] a) P. G. Bruce, S. A. Freunberger, L. J. Hardwick, J. M. Tarascon, *Nat. Mater.* **2012**, *11*, 19–29; b) M. Armand, J. M. Tarascon, *Nature* **2008**, *451*, 652; c) M. Milton, Q. Cheng, Y. Yang, C. Nuckolls, R. l. Hernández Sánchez, T. J. Sisto, *Nano Lett.* **2017**, *17*, 7859–7863.

[2] a) S. Xin, L. Gu, N.-H. Zhao, Y.-X. Yin, L.-J. Zhou, Y.-G. Guo, L.-J. Wan, *J. Am. Chem. Soc.* **2012**, *134*, 18510–18513; b) Y. Xu, Y. Wen, Y. Zhu, K. Gaskell, K. A. Cychosz, B. Eichhorn, K. Xu, C. Wang, *Adv. Funct. Mater.* **2015**, *25*, 4312–4320.

[3] X. Ji, K. T. Lee, L. F. Nazar, *Nat. Mater.* **2009**, *8*, 500–506.

[4] a) H. Wang, Y. Yang, Y. Liang, J. T. Robinson, Y. Li, A. Jackson, Y. Cui, H. Dai, *Nano Lett.* **2011**, *11*, 2644–2647; b) C. Wang, X. Wang, Y. Yang, A. Kushima, J. Chen, Y. Huang, J. Li, *Nano Lett.* **2015**, *15*, 1796–1802; c) R. Chen, T. Zhao, J. Lu, F. Wu, L. Li, J. Chen, G. Tan, Y. Ye, K. Amine, *Nano Lett.* **2013**, *13*, 4642–4649; d) N. Jayaprakash, J. Shen, S. S. Moganty, A. Corona, L. A. Archer, *Angew. Chem. Int. Ed.* **2011**, *50*, 5904–5908; *Angew. Chem.* **2011**, *123*, 6026–6030.

[5] a) Q. Pang, D. Kundu, M. Cuisinier, L. F. Nazar, *Nat. Commun.* **2014**, *5*, 4759; b) Y. Mi, W. Liu, K. R. Yang, J. Jiang, Q. Fan, Z. Weng, Y. Zhong, Z. Wu, G. W. Brudvig, V. S. Batista, H. Zhou, H. Wang, *Angew. Chem. Int. Ed.* **2016**, *55*, 14818–14822; *Angew. Chem.* **2016**, *128*, 15038–15042; c) G. Liang, J. Wu, X. Qin, M. Liu, Q. Li, Y.-B. He, J.-K. Kim, B. Li, F. Kang, *ACS Appl. Mater. Interfaces* **2016**, *8*, 23105–23113.

[6] a) Y.-S. Su, A. Manthiram, *Chem. Commun.* **2012**, *48*, 8817–8819; b) S. Evers, T. Yim, L. F. Nazar, *J. Phys. Chem. C* **2012**, *116*, 19653–19658; c) J. Song, M. L. Gordin, T. Xu, S. Chen, Z. Yu, H. Sohn, J. Lu, Y. Ren, Y. Duan, D. Wang, *Angew. Chem. Int. Ed.* **2015**, *54*, 4325–4329; *Angew. Chem.* **2015**, *127*, 4399–4403; d) S. H. Chung, A. Manthiram, *Adv. Mater.* **2014**, *26*, 7352–7357.

[7] a) Z. Wei Seh, W. Li, J. J. Cha, G. Zheng, Y. Yang, M. T. McDowell, P. C. Hsu, Y. Cui, *Nat. Commun.* **2013**, *4*, 1331; b) Y. Yuan, G. Tan, J. Wen, J. Lu, L. Ma, C. Liu, X. Zuo, R. Shahbazian-Yassar, T. Wu, K. Amine, *Adv. Funct. Mater.* **2018**, *28*, 1706443.

[8] a) H. Pan, J. Chen, R. Cao, V. Murugesan, N. N. Rajput, K. S. Han, K. Persson, L. Estevez, M. H. Engelhard, J.-G. Zhang, K. T. Mueller, Y. Cui, Y. Shao, J. Liu, *Nat. Energy* **2017**, *2*, 813–820; b) H. J. Peng, J. Q. Huang, X. Y. Liu, X. B. Cheng, W. T. Xu, C. Z. Zhao, F. Wei, Q. Zhang, *J. Am. Chem. Soc.* **2017**, *139*, 8458–8466.

[9] a) H. Pan, K. S. Han, M. Vijayakumar, J. Xiao, R. Cao, J. Chen, J. Zhang, K. T. Mueller, Y. Shao, J. Liu, *ACS Appl. Mater. Interfaces* **2017**, *9*, 4290–4295; b) H. Pan, K. S. Han, M. H. Engelhard, R. Cao, J. Chen, J. G. Zhang, K. T. Mueller, Y. Shao, J. Liu, *Adv. Funct. Mater.* **2018**, *28*, 1707234.

[10] S. Hess, M. Wohlfahrt-Mehrens, M. Wachtler, *J. Electrochem. Soc.* **2015**, *162*, A3084–A3097.

[11] H. Zhai, P. Xu, M. Ning, Q. Cheng, J. Mandal, Y. Yang, *Nano Lett.* **2017**, *17*, 3182–3187.

[12] a) B. Liu, J. Zhao, F. Wei, *J. Mol. Liq.* **2013**, *180*, 19–25; b) J. Wang, J. Han, M. Y. Khan, D. He, H. Peng, D. Chen, X. Xie, Z. Xue, *Polym. Chem.* **2017**, *8*, 1616–1627.

[13] a) E. Harder, V. M. Anisimov, T. Whitfield, A. D. MacKerell, B. Roux, *J. Phys. Chem. B* **2008**, *112*, 3509–3521; b) R. Hutcheon, J. Mouris, X. Fang, D. A. Scola, *Ceram. Trans.* **2001**, *111*, 109–118.

[14] P. Bazylewski, R. Divigalpitiya, G. Fanchini, *RSC Adv.* **2017**, *7*, 2964–2970.

[15] B. T. DiTullio, C. J. Wright, P. Hayes, P. J. Molino, T. W. Hanks, *Colloid Polym. Sci.* **2018**, *296*, 637–645.

[16] G.-C. Li, G.-R. Li, S.-H. Ye, X.-P. Gao, *Adv. Energy Mater.* **2012**, *2*, 1238–1245.

[17] G. He, X. Ji, L. Nazar, *Energy Environ. Sci.* **2011**, *4*, 2878.

[18] C. J. Bae, C. K. Erdonmez, J. W. Halloran, Y. M. Chiang, *Adv. Mater.* **2013**, *25*, 1254–1258.

[19] Z. Cao, P. Xu, H. Zhai, S. Du, J. Mandal, M. Dontigny, K. Zaghib, Y. Yang, *Nano Lett.* **2016**, *16*, 7235–7240.

[20] Y. Marcus, *Monatsh. Chem.* **2018**, *149*, 211–217.

Communications

Lithium–Sulfur Batteries

Q. Cheng, W. Xu, S. Qin, S. Das, T. Jin,
A. J. Li, A. C. Li, B. Qie, P. Yao, H. Zhai,
C. Shi, X. Yong, Y. Yang* ___ ◼◼◼◼–◼◼◼◼

Full Dissolution of the Whole Lithium
Sulfide Family (Li$_2$S$_8$ to Li$_2$S) in a Safe
Eutectic Solvent for Rechargeable
Lithium–Sulfur Batteries
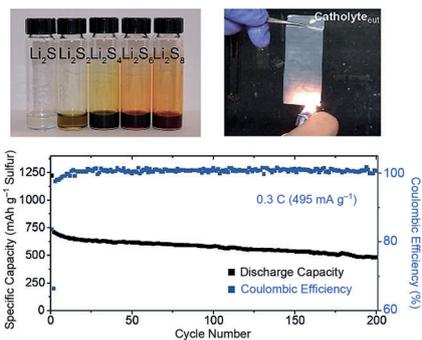
Electrolyte my fire: A new safe eutectic solvent of ε-caprolactam/acetamide can act as an electrolyte for lithium–sulfur batteries. It shows strong resistance to fire, and can dissolve the whole lithium sulfide family (Li$_2$S$_8$–Li$_2$S). It is low-cost and environmental friendly. By using this eutectic solvent, capacitance retentions of 68% over 200 cycles and 95% over 40 cycles were achieved with and without electrode modification, respectively.